Visualization of bacterial type 3 secretion system components down to the molecular level by MINFLUX nanoscopy

Alexander Carsten[1], Maren Rudolph[1], Tobias Weihs[2], Roman Schmidt[2], Christian A. Wurm[2], Andreas Diepold[3], Antonio Virgilio Failla[4], Manuel Wolters[1]*, Martin Aepfelbacher[1]*

1: Institute of Medical Microbiology, Virology and Hygiene, University Medical Center Hamburg Eppendorf, Martinistraße 52, 20251 Hamburg, Germany

2: Abberior Instruments GmbH, Hans Adolf Krebs Weg 1, 37077 Göttingen, Germany

3: Department of Ecophysiology, Max Planck Institute for Terrestrial Microbiology, Karl-von-Frisch-Str. 10, 35043 Marburg, Germany

4: UKE Microscopy Imaging facility, University Medical Center Hamburg Eppendorf, Martinistraße 52, 20251 Hamburg, Germany

*equal contribution

Correspondence: m.aepfelbacher@uke.de

Contact for questions concerning MINFLUX microscopy systems: c.wurm@abberior-instruments.com

Conceived and designed experiments: AC MR MW MA; Performed experiments: AC MR TW RS CAW MW; Analyzed the data: AC AVF; Contributed reagents/material/analysis tools/microscopes: TW RS CAW AD AVF; Wrote the paper: MA AC MW CAW AVF

Abstract

Type 3 secretion systems (T3SS) are essential virulence factors of numerous bacterial pathogens and inject effector proteins into host cells. The needle-like T3SS machinery consists of more than 20 components, has a length of around 100 nm and a diameter of up to 30 nm according to EM studies. Its intrabacterial components are highly dynamic and in permanent exchange with other bacterial structures. Therefore, a temporally and spatially resolved visualization of the T3SS using fluorescence microscopy techniques has been challenging. In the present study, novel labeling strategies were combined with super-resolution microscopy such as STED, STORM and MINFLUX. MINFLUX nanoscopy allowed to visualize components of the T3SS machinery such as the dynamic sorting platform component YscL and the extrabacterial pore protein YopD at unprecedented resolutions. The presented results represent the basis for an in depth investigation of T3SS structure and function and therefore gain new insights into the infection process of human pathogens in order to develop novel treatment and prevention strategies.

Introduction

Bacterial type III secretion systems (T3SSs)/injectisomes are central virulence factors of numerous human pathogens like *Pseudomonas*, EHEC, *Salmonella*, and *Yersinia* [1-3]. Injectisomes translocate bacterial effector proteins into host cells to manipulate a variety of cellular processes. The effectors are transported from the bacteria into the host cell through a hollow conduit that spans the inner and outer bacterial membranes and extrabacterial space and transitions into a pore complex/ translocon within the host cell membrane (Fig. 1 a).

Cryo-electron microscopy in combination with crystallography and biophysical techniques have provided molecular-resolution blueprints of T3SS needle complexes [4-8]. For single

particle analysis, needle complexes are purified from bacterial cultures. These lack translocons, which are formed only upon contact with the host cell, and sorting platforms (see below), which detach from the needle complexes during purification [9]. A recent cryo-electron tomography study visualized *Salmonella* translocons in situ. The translocons were embedded in the host cell membrane and displayed an outer diameter of ~13.5 nm and a thickness of ~8 nm [10].

Currently, it is assumed that two translocator proteins that make up the pore are transported through the injectisome needle and interact with the needle tip at its end. There, a protein complex, the so-called tip complex, is supposed to coordinate the integration of the translocators into the host cell membrane. The two translocators are thought to form a heteromultimeric (putatively hexadecameric 8:8 in *Pseudomonas*; [11]) ring structure with an inner opening of approximately 2 - 4 nm (Fig. 1 b and c) [7, 9-16]. However, until now functional T3SS pore complexes have not been reconstituted in vitro and none of the hydrophobic translocator proteins that form translocons have been crystallized [13, 15-18].

Cryo-electron tomography also allowed to visualize sorting platforms in their native environment. These structures are heteromultimeric protein assemblies, composed of the soluble T3SS sorting platform proteins YscL (SctL), YscQ (SctQ), YscK (SctK) and the ATPase YscN (SctN) (unified T3SS nomenclature [19, 20]), that dynamically interact with the cytoplasmic side of the injectisome and presumably control the targeting and secretion of T3SS substrates (Fig. 1 a, d and e) [4, 6, 21]. Cryo-electron tomography revealed significant structural differences between the *Salmonella*, *Chlamydia* and *Yersinia* sorting platforms. Intriguingly, the *Chlamydia* sorting platform and basal body were shown to undergo major conformational changes upon contact with the host cell, whereas this was not observed for the *Yersinia* or *Salmonella* T3SS [4, 10, 21]. In summary, the structure of the sorting platform

and the injectisome have been resolved using electron microscopy. However, due to the applied methods, information on the molecular basis and functional significance of the observed structural differences and conformational changes, while intriguing, are not yet understood.

Thus, many questions regarding assembly, structure, function and control of translocons and the sorting platform have remained unresolved to date. Their clarification amongst others requires new imaging methods that combine the highest spatial resolution with molecular specificity.

The developments in fluorescence nanoscopy in the last two decades have allowed for the first time to satisfactorily visualize subcellular structures in bacterial cells [22-25]. Two approaches have proven to be particularly suitable and promising in this context, achieving resolution ranges of 20 – 70 nm [26]. One approach is based on the direct recording of super resolved images and includes stimulated emission depletion (STED) microscopy and reversible saturable optical fluorescence transitions (RESOLFT) nanoscopy [27, 28]. Another approach is single molecule localization microscopy (SMLM) that includes PALM (photoactivation localization microscopy) and STORM (stochastic optical reconstruction microscopy) [29; 30]. Recently, minimal photon flux (MINFLUX) nanoscopy has been developed that combines the specific strengths of STED and PALM/STORM [31-33]. In MINFLUX, the localization of individual fluorophores is determined by actively directing a donut-shaped excitation beam with a central intensity minimum to the fluorophore and triangulating its position. This approach allows to use the limited photon-budget of a fluorophore more efficiently and with 1 – 5 nm achieves the highest localization precision of all nanoscopy methods known to date [32, 33].

PALM nanoscopy was previously employed to visualize several labeled components of sorting platform and export apparatus and to estimate their stoichiometry in injectisomes [25, 34]. Nauth et al. recently employed SIM and STED nanoscopy to image basal body and translocator proteins of the *Yersinia enterocolitica* injectisome during host cell infection [23]. The translocators YopB and YopD could be visualized inserted into a phosphatidylinositol-4,5-bisphosphate (PI(4,5)P2) membrane compartment at 80 - 90 nm lateral and 100 nm axial resolution. YopB and YopD thereby co-localized with the tip-complex protein LcrV, suggesting that the translocators are part of assembled translocons associated with the needle tip. Moreover, the distance of the YopB/D signals in the translocon to more proximal GFP-YscD signals within the basal body could be determined to be 109 nm [23].

Fluorescence imaging of proteins at a resolution level well below 10 nm has become feasible with MINFLUX. However, in antibody-based detection methods a maximum offset between the label from the target protein of up to two antibody lengths, i.e. by around 15 nm has to be taken into account. To make use of the full resolution of the MINFLUX microscope, we decided to apply an adapted labeling strategy for the investigated proteins [26]. Small affinity probes like nanobodies or aptamers coupled to fluorophores with a total length of around 5 nm have been successfully applied in this regard [35-37]. When considering to label proteins that are crucial for a specific bacterial function, in situ genome editing methods are advantageous over transient expression from plasmids, because the latter may result in non-physiological expression levels that can potentially affect function and distribution of the respective proteins at the nanoscale level [38]. Furthermore, if components of the T3SS, especially effector and translocator proteins, are to be fused with heterologous proteins, it must be considered that the secretion signal must be preserved, and that certain tertiary structures are incompatible with the protein unfolding processes required for protein

secretion and could also interfere with membrane integration of translocator proteins [39-41].

The aim of this work was to use MINFLUX nanoscopy to investigate the YopD translocator and the sorting platform component YscL of the *Y. enterocolitica* injectisome in their native environment using the exceptionally resolution down to the single molecule level. To this end, a 13 amino acid nanobody-binding peptide tag (ALFA tag) was genetically engineered into endogenous YopD at an internal position, such that it did not interfere with translocation or function of the protein [42]. The sorting platform protein YscL was investigated in a previously established strain carrying YscL fused with the self-labeling Halo-tag [43].

Results and discussion

Presently there is no high-resolution structure of the T3SS translocon or a realistic modeling of its assembly process available. It appears that the two hydrophobic translocator proteins, after their passage through the needle, integrate into the host cell membrane and assemble the translocon, but their interplay and stoichiometry in the translocon are unclear.

In order to analyze translocons at high spatial and temporal resolution using fluorescence microscopy, a function-preserving labeling of the translocators suitable for super-resolution microscopy and live cell imaging is required. To take a step toward this goal, we used CRISPR-Cas assisted recombineering to insert into the translocator YopD a 15 amino acid ALFA-tag in situ, i.e., in the background of the wild type strain WA-314, giving rise to WA-314 YopD-ALFA (Methods, Fig. 1 f). The ALFA tag was inserted between amino acids 194 and 195 in YopD because this position should not affect the N-terminal motifs required for secretion and translocation (aa 1 to 15) [44], the predicted transmembrane domain (aa 128 to 149) [45] or

the putative interaction sites of YopD with YopB or LcrV [46] (Fig. 1 f). The YopD interaction sites were estimated from studies mapping the analogous interactions sites of the highly homologous translocator PopD from *P. aeruginosa* [46]. The ALFA tag was chosen because it can be bound with low picomolar affinity by a fluorescently labeled nanobody (NbALFA), which positions the fluorescent label within ~5 nm of the ALFA-tagged protein (Fig. 1 b and c) [44].

We sought to verify that the functionality of WA-314 YopD-ALFA was preserved. First, YopD-ALFA extracted from HeLa cells infected with WA-314 YopD-ALFA coprecipitated with YopB, indicating that YopD-ALFA becomes translocated and interacts with YopB (Fig. 1 g). Secondly, when WA-314 YopD-ALFA infected HeLa cells were imaged with STED nanoscopy YopD-ALFA and YopB colocalized in spot-like structures identified as translocons in previous work (Fig. 1 h) [23]. Thirdly, WA-314 and WA-314 YopD-ALFA translocated virtually identical levels of YopD and YopD-ALFA, respectively, as well as the effector YopH into Hela cells (Fig. 1 i). Overall, these data demonstrate that insertion of the ALFA tag into YopD in WA-314 enables NbALFA-based staining of translocons during cell infection while not interfering with YopD function.

Next, we compared the resolution of different super-resolution microscopy techniques when imaging translocon-associated YopD-ALFA. For this STED-, STORM- and MINFLUX nanoscopy were performed with fixed and permeabilized WA-314 YopD-ALFA infected Hela cells stained with NbALFA (Fig. 1 b) coupled to suitable fluorophores (Abberior STAR 635P for STED nanoscopy or Alexa Fluor 647 for STORM and MINFLUX nanoscopy) (Fig. 2 a and b). For better orientation, in parallel to STED and MINFLUX nanoscopy YopD-ALFA was imaged with confocal microscopy and in parallel to STORM nanoscopy with epifluorescence microscopy. Confocal and epifluorescence microscopy revealed partly confluent patches of YopD-ALFA signals at the bacterial cell periphery (Fig. 2 a). In comparison, STORM- and STED microscopy further

resolved the YopD-ALFA signals into distinct spots (Fig. 2 a). The lateral extents of the fluorescence signals detected by STED and STORM nanoscopy were in the range of 50 nm as compared to ~250-300 nm measured with the diffraction limited microscopy methods. (Fig. 2 a i-vi). MINFLUX nanoscopy, which provided a localization precision of $\sigma\tilde{} < 5$ nm (median value in the raw data) in our samples, revealed significantly smaller structures (Fig. 2 a vii-ix and b). These structures regularly appeared as clusters of up to 3 separable signals (Fig. 2 b). To estimate the extent of these clusters, the largest lateral diameter of the clusters was determined, yielding a mean value of about 28 nm (FWHM). Considering the obtained localization precision of the used MINFLUX technology and the linkage error generated by the fluorescent NbALFA (up to 2 x ~5 nm, Fig. 1 b and c), we suggest that the clusters represent single translocons as described previously [23] and we propose that the separate signals in the clusters represent single YopD-ALFA subunits within translocons. With 28 nm the estimated mean of the largest lateral diameters of the clusters is relatively close to the 14 nm diameter determined by cryo-electron tomography for the *Salmonella* translocon [10]. For better illustration, recordings of MINFLUX YopD-ALFA clusters were overlayed with a schematic model based on the proposed hexadecameric (8/8) stoichiometry [11] and the dimensions of the Salmonella translocon [10] (Fig. 2 b). Of note, we detected only up to 3 individual signals per cluster (26 clusters evaluated). This is less than the 8 copies of YopD per translocon as would be inferred from the model of the *P. aeruginosa* translocon [11]. Possible explanations for this apparent discrepancy may be incomplete labeling of YopD-ALFA by the nanobody, confluence of laterally (x/y) closely spaced signals or overlap of signals along the optical axis (z).

We next aimed at imaging the T3SS sorting platform component YscL with super-resolution fluorescence microscopy. In a recent cryo-electron tomography study of the *Y. enterocolitica*

T3SS, YscL was shown to form a bowl shaped structure of ~16 nm in diameter composed of a hexamer of YscL dimers [4]. To visualize this structure, an established *Y. enterocolitica* strain E40ΔHOPEMT Halo-YscL harboring YscL N-terminally fused with the self-labeling enzyme tag Halo was employed (Fig. 1 d and e) [43]. Labeling with the Halo-tag allows for a highly specific fluorescence staining whereby the enzymatic activity of Halo catalyzes a covalent binding to fluorescent substrates [47]. E40ΔHOPEMT Halo-YscL grown under T3SS inducing conditions (Methods), fixed and stained with Alexa Fluor 647-labeled Halo substrate and imaged by STORM and MINFLUX nanoscopy. For orientation, Halo-YscL was in parallel imaged with confocal (MINFLUX) or epifluorescence (STORM) microscopy yielding a rather homogenous signal with slightly increased intensity at the periphery of the bacteria (Fig. 2 c v). STORM nanoscopy provided a more detailed image resolving distinct signals, which partly overlapped (Fig. 2 c, zoom). In comparison, MINFLUX microscopy recorded images with a localization precision of $\sigma < 5$ nm (median value in raw data) revealing separate, point-like signals with a lateral extent in the range of 15 - 20 nm. As shown in Fig. 2 c, the MINFLUX Halo-YscL signals fit well to the size of the bowl-shaped dodecamer formed by YscL as determined by cryo-electron tomography (indicated in red; adapted from [4]). The Halo-YscL proteins in sorting platforms yielded rather dense and homogeneous signals by MINFLUX nanoscopy, which is in contrast to the individual MINFLUX signals apparently representing single YopD-ALFA proteins in translocons (Fig. 2 b). This finding might be related to the higher copy number of YscL per injectisome (most likely 12 copies of YscL per sorting platform [25, 43, 48]) in combination with more efficient fluorescent labeling of the Halo-tagged YscL as compared to the nanobody based staining of YopD-ALFA or the orientation of the Halo-tag in the complex, which has not yet been established.

In summary, we conclude that MINFLUX nanoscopy enables imaging of translocon-associated YopD and sorting platform-associated YscL with a hitherto unprecedented lateral localization precision of < 5 nm (median in raw data). The MINFLUX technique used in this work resolved bacterial structures that most likely represent single proteins in the case of the translocon component YopD or large protein complexes in the case of YscL in sorting platforms. An important limitation to the MINFLUX data shown in this study is that the applied 2D MINFLUX system provides only confocal resolution along the optical axis (> 600 nm), while a lateral localization precision in the range of a few nanometers is achieved. In turn, this complicates interpretation of the images because differently oriented structures yield differently shaped signals in a single-layer 2-D image

Altogether, the MINFLUX nanoscopy platform is rapidly evolving and systems offering nanometer resolution in three dimensions and two-color registration have already been reported [32]. Future studies using these advanced systems will likely provide an even more detailed picture of the dimensions and composition of the T3SSs, e.g. by parallel three-dimensional imaging of two or more T3SS components or even live cell imaging technologies.

Methods and Materials

All standard laboratory chemicals and supplies were purchased from Roth (Karlsruhe, Germany), Sigma-Aldrich (Steinheim, Germany) or Merck (Hohenbrunn, Germany) unless indicated otherwise.

Plasmids

The following plasmids were described previously: pKD46-Cas12a and pAC-crRNA plasmids [49] were provided by Yi-Cheng Sun (MOH Key Laboratory of Systems Biology of Pathogens, Institute of Pathogen Biology, and Center for Tuberculosis Research, Chinese Academy of Medical Sciences and Peking Union Medical College, Beijing, China). The myc-Rac1Q61L plasmid was kindly provided by Dr. Pontus Aspenström (Uppsala University, Uppsala, Sweden).

Oligonucleotides

YopD-ALFA HomA fwd	TATTATCCTAACTTATTATTTTTAATTTAATAATAAAAGCCCTGGATTACCA TTAGTTAA
YopD-ALFA HomA rev	TTGGAAGAGGAACTGAGACGCCGCTTAACTGAACCAGGCGGAGGTGGAT CTATCGGGAGAATATGGAAACCAGA
YopD-ALFA HomB fwd	GCGGCGTCTCAGTTCCTCTTCCAAACGGCTCGGGCCACCAGACCCGCCCG AACCACCATCCTCTCTGCTTACCGCTTTAT
YopD-ALFA HomB rev	AAAGCGGTGAGGTTAAAAAAA
YopD-crRNA fwd	TAGATCATATTCTCCCGATATCCTC
YopD-crRNA rev	AGACGAGGATATCGGGAGAATATGA

Antibodies and nanobodies

The following primary antibodies were used: Polyclonal rabbit anti-YopB polyclonal and rabbit anti-YopD [23]. Anti-YopH rabbit polyclonal serum was a gift of Jürgen Hesemann (Max von Pettenkofer-Institute, Munich, Germany). Rabbit polyclonal anti-calnexin (Enzo, Lörrach, Germany).

Secondary anti-IgG antibodies and their sources were: Alexa Fluor Plus 594 goat anti-rabbit antibody (Invitrogen, Rockford, USA). Horseradish peroxidase linked donkey anti-rabbit (GE Healthcare, Chicago, USA).

Conjugated primary camelid anti-ALFA nanobodies (NbALFA) and their source were: Abberior®STAR 635P FluoTag®-X2, Alexa Fluor 647 FluoTag®-X2, HRP FluoTag®-X2 (NanoTag Biotechnologies, Göttingen, Germany).

Source and generation of Yersinia mutants

Y. enterocolitica wild type strain WA-314 was a gift of Jürgen Heesemann (Max von Pettenkofer Institute, Munich, Germany) and described previously [50]. *Y. enterocolitica* E40 derived mutant strain ADTM4525 pYV40ΔYopOEHMPTΔasd halo-yscL (here designated: E40ΔOEHMPT Halo-YscL) construction and characterization was described previously [43].

WA-314 YopD-ALFA was generated using a CRISPR-Cas12a-assisted recombineering approach as described previously [49]. In brief, a double stranded Homology Directed Repair (HDR) fragment containing the ALFA-tag sequence was generated via overlap extension PCR. For this a 500 bp homology arm (HomA) was amplified from the *Y. enterocolitica* pYV virulence plasmid with the reverse primer YopD-ALFA HomA rev including part of the ALFA-tag insert and linker and the corresponding forward primer YopD-ALFA HomA fwd. The other homology arm (HomB) was amplified using the forward primer YopD-ALFA HomB fwd including the remaining part of the ALFA-tag insert and linker and the corresponding reverse primer YopD-ALFA HomB rev. Both homology arms were used as templates in an overlap extension PCR using the outer primers (YopD-ALFA HomA fwd and YopD-ALFA HomB rev) to generate the final HDR fragment.

The crRNAs required for targeting Cas12a to the definded insertion site were designed based on the 20 bp protospacer following the 3'-end of a PAM (5'-TTN-3'). The respective

oligonucleotides were designed with Eco31L overhangs at the 5'- and 3'-ends (YopD-crRNA fwd and YopD-crRNA rev), annealed and ligated into the Eco31L digested pAC-crRNA vector harboring also a sacB sucrose sensitivity gene. 700 ng of the HDR fragment and 350 ng of the pAC-crRNA were electroporated into an electrocompetent WA-314 strain carrying pKD46-Cas12a, which harbors the lambda Red recombinase under control of an arabinose inducible promotor, Cas12a (Cas12a/Cpf1 from *Francisella novicida*) and a temperature-sensitive replicon. After successful editing of the virulence plasmid, the pAC-crRNA and pKD46-Cas12a plasmids were cured from the bacteria. Correct insertion of the ALFA-tag was confirmed by PCR and sequencing.

Cell culture and transfection

HeLa cells (ACC#57, DSMZ-German Collection of Microorganisms and Cell Cultures) were cultured at 37 °C and 5% CO_2 in DMEM (Invitrogen, GIBCO, Darmstadt, Germany) supplemented with 10% FCS. For infection with bacteria, HeLa cells were seeded in 6 well plates (3 x 10^5 cells per well) or on glass coverslips (STED: 12mm, No. 1.5H for high resolution, Marienfeld GmbH, Lauda-Königshafen, Germany, density 6 x $10^{4;}$ STORM/MINFLUX: 18 mm, No. 1.5H, Marienfeld GmbH, Lauda-Königshafen, Germany, density 3 x 10^5). HeLa cells were transfected with 0.25 µg/6 x 10^4 Hela cells of the myc-Rac1Q61L plasmid with turbofect (Thermo Fisher Scientific, Waltham, Massachusetts, USA) for 16 h according to the manufacturer's protocol.

Preparation of bacteria

Yersinia were grown in LB broth (WA-314 and WA-314 YopD-ALFA) supplemented with nalidixic acid and kanamycin as required; E40ΔOEHMPT Halo-YscL supplemented with nalidixic acid, arsenite and diaminopimelic acid at 27 °C overnight and then diluted 1:20 in fresh LB

broth, followed by cultivation at 37 °C for 1.5 h to induce expression of the T3SS. These cultures were also used for cell infection experiments (see below). For *in-vitro* Yop secretion, EGTA was added to the growth medium (Ca^{++}-depletion), followed by another 3 h of incubation at 37 °C, as described [51].

For cell infection, bacteria were centrifuged, resuspended in ice-cold PBS and added to target cells at a defined multiplicity of infection (MOI), as specified in the figure captions. Bacteria were then centrifuged at 200 x g for 1 min onto the target cells to synchronize bacterial attachment.

Fluorescence labeling

Cell-associated bacteria were fixed with 4% formaldehyde (prepared from PFA; Electron Microscopy Science, Hatfield, USA) in PBS for 5 - 10 min and then treated with digitonin solution (90 µg/mL in PBS) to allow fluorescently labeled NbALFA access translocon-associated but not intrabacterial YopD-ALFA. Bacteria grown under *in-vitro* Yop secretion conditions were fixed with 4% formaldehyde in PBS for 5-10 min and then treated with 0.005% Triton X-100 in PBS to allow the fluorescently labeled Halo-tag substrate to access the intrabacterial Halo-YscL proteins. Unspecific binding sites were blocked with 3% bovine serum albumin (BSA, w/v) in PBS for at least 45 min.

Depending on the microscopy method samples were then incubated with different dilutions of fluorescently labeled FluoTag®-X2 anti-ALFA nanobody in 3% BSA/PBS (STED: 1:200 dilution for 16 h, NbALFA coupled to Abberior STAR 635P; STORM and MINFLUX: 1:1500 dilution for 1 to 2 h, NbALFA coupled to Alexa Fluor 647) or HaloTag® Fluorescent Ligand (Promega, Walldorf, Germany) coupled to Alexa Fluor 647 (STORM and MINFLUX: 0.25 µM for 16 h) (Invitrogen, Rockford, USA). Samples incubated with primary rabbit anti-YopB antibody (STED:

1:50 for 1 h) were washed three times with PBS and then incubated with a 1:200 dilution of anti-rat secondary antibody coupled to Alexa Fluor Plus 594 for at least 2 h. After staining with the respective fluorescent labels, samples were washed multiple times with PBS.

Sample mounting and imaging buffers

STED samples were mounted in ProLong Gold (Thermo Fisher Scientific, Waltham, USA). For STORM imaging the "Smart kit for STORM" (Abbelight, Cachan, France) was used according to manufacturer's protocol. For MINFLUX imaging, gold nanorods (Nanopartz Inc., A12-40-980-CTAB-DIH-1-25) were used as fiducials and a GLOX buffer was used for imaging (both described in [33]). STORM and MINFLUX samples were sealed with twinsil (picodent, Wipperfürth, Germany).

Microscopy and super-resolution imaging

STED nanoscopy and corresponding confocal microscopy were carried out in line sequential mode using an Abberior Instruments Expert Line STED microscope based on a Nikon Ti-E microscopy body and employed for excitation and detection of the fluorescence signal a 60x Plan APO 1.4 oil immersion objective. A pulsed 640 nm laser was used for excitation and a pulsed near-infrared laser (775 nm) was used for STED. The detected fluorescence signal was directed through a variable sized pinhole (1 Airy unit at 640 nm) and detected by avalanche photo diodes (APDs) with appropriate filter settings for Cy5 (615 - 755 nm). Images were recorded with a dwell time of 0.5 µs and the pixel size was set to be 10 nm. The acquisitions were carried out in time gating mode i.e. with a time gating delay of 750 ps and a width of 8 ns. STED images were acquired with a 2D-STED donut.

STORM nanoscopy and corresponding epifluorescence microscopy were carried out using a Abbelight SAFe 180 setup based on an Olympus IX-81 microscopy body and employed for

excitation and detection of the fluorescence signal a 100x UPlan Apo HR TIRF oil immersion objective with a pixel size of 78 nm. A solid-state 640 nm laser was used for excitation (10% laser intensity for epifluorescence imaging; 70% laser intensity for STORM imaging). The detected fluorescence signal was recorded by a Hamamatsu ORCA Flash 4.0 V2 camera. 10,000 frames at 50 ms exposure time were acquired for reconstruction of the STORM image. Resulting coordinate tables and images were processed using Abbelight SAFe NEO software. MINFLUX nanoscopy, corresponding confocal microscopy and image rendering were carried out using a MINFLUX setup previously described in[33].

Determination of the FWHM of single translocon fluorescence signals

Single translocon clusters were identified (representatively shown in Fig. 2a viii) and Fig. 2b)). The largest lateral extent of the MINFLUX signal was determined and a plot profile line was drawn (representatively shown in Fig. 2a viii)). 26 single translocons of different bacteria were measured, averaged and plotted and the FWHM was determined.

Detection of released effector and translocator proteins

Released effector (YopH) and translocator proteins (YopB/D) were analyzed as described previously [52]. In brief, HeLa cells were infected with a MOI of 100 for 60 min and subsequently washed with PBS to remove non-adherent bacteria. HeLa cells were lysed by the addition of digitonin (0.5% w/v in PBS) at room temperature for 20 min, with repeated vortexing. Cell debris and attached bacteria were separated from the lysate containing the released effectors by centrifugation. The resulting supernatants were analyzed by SDS-PAGE, transferred to a PVDF membrane (Immobilon-P, Millipore) and analyzed by Western blot using antisera against YopH, YopB and YopD, antibodies against calnexin and HRP-coupled NbALFA.

Pull down assay

Per condition 30 µl of ALFA Selector ST slurry (NanoTag Biotechnologies, Göttingen, Germany) were washed with 1 ml of cold PBS containing protease inhibitor. For each condition two confluent 10 cm cell culture dishes of HeLa cells were infected (MOI: 100; 1 h). Hela cells were treated with 1 µg/ml CNF-1 for 2 h before infection as specified in the figure captions to increase Yop translocation [53]. Infected cells were washed once with PBS before adding 750 µl 0.5 % digitonin in PBS containing protease inhibitor per dish. Infected cells were scraped from the dish and centrifuged (14 000 x *g*, 4 °C, 10 min). A 60 µL sample (lysate) was taken and the remaining supernatant was transferred to the beads and incubated for 1.5 h at 4 °C on a rotor. After centrifugation (1000 x *g*, 4 °C, 2 min) a 60 µL sample (supernatant) was taken. The beads were resuspended in PBS containing protease inhibitor, transferred into a fresh reaction tube and washed three times with 1 ml PBS containing protease inhibitor. The beads were resuspended in 30 µl SDS buffer and incubated for 7 min at 95 °C (pull down).

Acknowledgements

This study was supported by the Joachim Herz Foundation given to Alexander Carsten. We thank the UKE microscopy Imaging facility (umif) for training and support especially during STORM acquisitions.

The authors declare the following competing interests. R.S., T.W. and C.A.W. are employees of Abberior Instruments manufacturing MINFLUX microscopes. C.A.W. is employee of Abberior commercializing fluorophores for super resolution. C.A.W. holds shares of Abberior Instruments. The other authors declare no competing interests.

References:

1. Lara-Tejero, M. and J.E. Galan, *The Injectisome, a Complex Nanomachine for Protein Injection into Mammalian Cells.* EcoSal Plus, 2019. **8**(2).
2. Pinaud, L., P.J. Sansonetti, and A. Phalipon, *Host Cell Targeting by Enteropathogenic Bacteria T3SS Effectors.* Trends Microbiol, 2018. **26**(4): p. 266-283.
3. Deng, W., et al., *Assembly, structure, function and regulation of type III secretion systems.* Nat Rev Microbiol, 2017. **15**(6): p. 323-337.
4. Berger, C., et al., *Structure of the Yersinia injectisome in intracellular host cell phagosomes revealed by cryo FIB electron tomography.* J Struct Biol, 2021. **213**(1): p. 107701.
5. Lunelli, M., et al., *Cryo-EM structure of the Shigella type III needle complex.* PLoS Pathog, 2020. **16**(2): p. e1008263.
6. Hu, J., et al., *Cryo-EM analysis of the T3S injectisome reveals the structure of the needle and open secretin.* Nat Commun, 2018. **9**(1): p. 3840.
7. Worrall, L.J., et al., *Near-atomic-resolution cryo-EM analysis of the Salmonella T3S injectisome basal body.* Nature, 2016. **540**(7634): p. 597-601.
8. Marlovits, T.C., et al., *Structural insights into the assembly of the type III secretion needle complex.* Science, 2004. **306**(5698): p. 1040-2.
9. Mueller, C.A., et al., *The V-antigen of Yersinia forms a distinct structure at the tip of injectisome needles.* Science, 2005. **310**(5748): p. 674-6.
10. Park, D., et al., *Visualization of the type III secretion mediated Salmonella-host cell interface using cryo-electron tomography.* Elife, 2018. **7**.
11. Romano, F.B., et al., *Type 3 Secretion Translocators Spontaneously Assemble a Hexadecameric Transmembrane Complex.* J Biol Chem, 2016. **291**(12): p. 6304-15.
12. Akopyan, K., et al., *Translocation of surface-localized effectors in type III secretion.* Proc Natl Acad Sci U S A, 2011. **108**(4): p. 1639-44.
13. Hakansson, S., et al., *The YopB protein of Yersinia pseudotuberculosis is essential for the translocation of Yop effector proteins across the target cell plasma membrane and displays a contact-dependent membrane disrupting activity.* EMBO J, 1996. **15**(21): p. 5812-23.
14. Holmstrom, A., et al., *YopK of Yersinia pseudotuberculosis controls translocation of Yop effectors across the eukaryotic cell membrane.* Mol Microbiol, 1997. **24**(1): p. 73-91.
15. Montagner, C., C. Arquint, and G.R. Cornelis, *Translocators YopB and YopD from Yersinia enterocolitica form a multimeric integral membrane complex in eukaryotic cell membranes.* J Bacteriol, 2011. **193**(24): p. 6923-8.
16. Neyt, C. and G.R. Cornelis, *Insertion of a Yop translocation pore into the macrophage plasma membrane by Yersinia enterocolitica: requirement for translocators YopB and YopD, but not LcrG.* Mol Microbiol, 1999. **33**(5): p. 971-81.
17. Blocker, A., et al., *The tripartite type III secreton of Shigella flexneri inserts IpaB and IpaC into host membranes.* J Cell Biol, 1999. **147**(3): p. 683-93.
18. Ide, T., et al., *Characterization of translocation pores inserted into plasma membranes by type III-secreted Esp proteins of enteropathogenic Escherichia coli.* Cell Microbiol, 2001. **3**(10): p. 669-79.
19. Wagner, S. and A. Diepold, *A Unified Nomenclature for Injectisome-Type Type III Secretion Systems.* Curr Top Microbiol Immunol, 2020. **427**: p. 1-10.
20. Hueck, C.J., *Type III protein secretion systems in bacterial pathogens of animals and plants.* Microbiol Mol Biol Rev, 1998. **62**(2): p. 379-433.

21. Nans, A., et al., *Structure of a bacterial type III secretion system in contact with a host membrane in situ.* Nat Commun, 2015. **6**: p. 10114.
22. Vojnovic, I., J. Winkelmeier, and U. Endesfelder, *Visualizing the inner life of microbes: practices of multi-color single-molecule localization microscopy in microbiology.* Biochem Soc Trans, 2019. **47**(4): p. 1041-1065.
23. Nauth, T., et al., *Visualization of translocons in Yersinia type III protein secretion machines during host cell infection.* PLoS Pathog, 2018. **14**(12): p. e1007527.
24. Heesemann J, Laufs R. Construction of a mobilizable Yersinia enterocolitica virulence plasmid. *J Bacteriol*. 1983;155:761–7.
25. Zhang, Y., et al., *Visualization and characterization of individual type III protein secretion machines in live bacteria.* Proc Natl Acad Sci U S A, 2017. **114**(23): p. 6098-6103.
26. Sahl, S.J., S.W. Hell, and S. Jakobs, *Fluorescence nanoscopy in cell biology.* Nat Rev Mol Cell Biol, 2017. **18**(11): p. 685-701.
27. Hell, S.W. and J. Wichmann, *Breaking the diffraction resolution limit by stimulated emission: stimulated-emission-depletion fluorescence microscopy.* Opt Lett, 1994. **19**(11): p. 780-2.
28. Hofmann, M., et al., *Breaking the diffraction barrier in fluorescence microscopy at low light intensities by using reversibly photoswitchable proteins.* Proc Natl Acad Sci U S A, 2005. **102**(49): p. 17565-9.
29. Betzig, E., et al., *Imaging intracellular fluorescent proteins at nanometer resolution.* Science, 2006. **313**(5793): p. 1642-5.
30. Rust, M.J., M. Bates, and X. Zhuang, *Sub-diffraction-limit imaging by stochastic optical reconstruction microscopy (STORM).* Nat Methods, 2006. **3**(10): p. 793-5.
31. Balzarotti, F., et al., *Nanometer resolution imaging and tracking of fluorescent molecules with minimal photon fluxes.* Science, 2017. **355**(6325): p. 606-612.
32. Gwosch, K.C., et al., *MINFLUX nanoscopy delivers 3D multicolor nanometer resolution in cells.* Nat Methods, 2020. **17**(2): p. 217-224.
33. Schmidt, R., et al., *MINFLUX nanometer-scale 3D imaging and microsecond-range tracking on a common fluorescence microscope.* Nat Commun, 2021. **12**(1): p. 1478.
34. Diepold, A., et al., *Composition, formation, and regulation of the cytosolic c-ring, a dynamic component of the type III secretion injectisome.* PLoS Biol, 2015. **13**(1): p. e1002039.
35. Ries, J., et al., *A simple, versatile method for GFP-based super-resolution microscopy via nanobodies.* Nat Methods, 2012. **9**(6): p. 582-4.
36. Pleiner, T., et al., *Nanobodies: site-specific labeling for super-resolution imaging, rapid epitope-mapping and native protein complex isolation.* Elife, 2015. **4**: p. e11349.
37. Mikhaylova, M., et al., *Resolving bundled microtubules using anti-tubulin nanobodies.* Nat Commun, 2015. **6**: p. 7933.
38. Gibson, T.J., M. Seiler, and R.A. Veitia, *The transience of transient overexpression.* Nat Methods, 2013. **10**(8): p. 715-21.
39. Radics, J., L. Konigsmaier, and T.C. Marlovits, *Structure of a pathogenic type 3 secretion system in action.* Nat Struct Mol Biol, 2014. **21**(1): p. 82-7.
40. Lee, V.T. and O. Schneewind, *Yop fusions to tightly folded protein domains and their effects on Yersinia enterocolitica type III secretion.* J Bacteriol, 2002. **184**(13): p. 3740-5.
41. Akeda, Y. and J.E. Galan, *Chaperone release and unfolding of substrates in type III secretion.* Nature, 2005. **437**(7060): p. 911-5.

42. Gotzke, H., et al., *The ALFA-tag is a highly versatile tool for nanobody-based bioscience applications.* Nat Commun, 2019. **10**(1): p. 4403.
43. Diepold, A., et al., *A dynamic and adaptive network of cytosolic interactions governs protein export by the T3SS injectisome.* Nat Commun, 2017. **8**: p. 15940.
44. Amer, A.A., et al., *Impact of the N-terminal secretor domain on YopD translocator function in Yersinia pseudotuberculosis type III secretion.* J Bacteriol, 2011. **193**(23): p. 6683-700.
45. Mattei, P.J., et al., *Membrane targeting and pore formation by the type III secretion system translocon.* FEBS J, 2011. **278**(3): p. 414-26.
46. Armentrout, E.I. and A. Rietsch, *The Type III Secretion Translocation Pore Senses Host Cell Contact.* PLoS Pathog, 2016. **12**(3): p. e1005530.
47. Los, G.V., et al., *HaloTag: a novel protein labeling technology for cell imaging and protein analysis.* ACS Chem Biol, 2008. **3**(6): p. 373-82.
48. Bernal, I., et al., *Molecular Organization of Soluble Type III Secretion System Sorting Platform Complexes.* J Mol Biol, 2019. **431**(19): p. 3787-3803.
49. Yan, M.Y., et al., *CRISPR-Cas12a-Assisted Recombineering in Bacteria.* Appl Environ Microbiol, 2017. **83**(17).
50. Oellerich, M.F., et al., *Yersinia enterocolitica infection of mice reveals clonal invasion and abscess formation.* Infect Immun, 2007. **75**(8): p. 3802-11.
51. Heesemann, J., et al., *Immunochemical analysis of plasmid-encoded proteins released by enteropathogenic Yersinia sp. grown in calcium-deficient media.* Infect Immun, 1986. **54**(2): p. 561-7.
52. Nordfelth, R. and H. Wolf-Watz, *YopB of Yersinia enterocolitica is essential for YopE translocation.* Infect Immun, 2001. **69**(5): p. 3516-8.
53. Wolters, M., et al., *Cytotoxic necrotizing factor-Y boosts Yersinia effector translocation by activating Rac protein.* J Biol Chem, 2013. **288**(32): p. 23543-53.
54. Pallen, M.J., G. Dougan, and G. Frankel, *Coiled-coil domains in proteins secreted by type III secretion systems.* Mol Microbiol, 1997. **25**(2): p. 423-5.
55. Hakansson, S., et al., *YopB and YopD constitute a novel class of Yersinia Yop proteins.* Infect Immun, 1993. **61**(1): p. 71-80.

Figure captions

Fig. 1: Schematic representations of the T3SS and characterization of WA-314 YopD-ALFA

(a) Schematic representation of the *Y. enterocolitica* type 3 secretion system. IM, inner membrane; PG, peptidoglycan layer; OM, outer membrane; HCM, host cell membrane; Scale bar: 20 nm. Adapted from [4, 10].

(b, c) Schematic representation of fluorescent NbALFA bound YopD-ALFA in the pore complex. Nb, fluorescent NbALFA binding ALFA-tag. Dimension of the *Y. enterocolitica* pore complex was derived from the dimension of the *S. typhimurium* pore complex [10]. Putative number and organization of YopD and YopB proteins in the *Y. enterocolitica* pore complex were derived from the putative number and organization of the PopD and PopB proteins in the *P. aeruginosa* pore complex [11]. Length of the fluorescent NbALFA is about 5 nm [42]. (b): side view; (c): top view.

(d, e) Schematic representation of Halo-YscL localization in the sorting platform. Sorting platform dimension was derived from [4]. (d): side view; (e): bottom view.

(f) Schematic representation of ALFA-tagged YopD. Virtual YopD protein. Amino acid (aa) numbers and regions of YopD are from different *Yersinia* strains. SEC, secretion signal (aa 1-15, in *Y. pseudotuberculosis* [44]); TM, transmembrane region (aa 128-149, in *Yersinia* spp. [45]); ALFA-tag with linkers (28 aa) inserted between aa 194 and 195; CC, coiled coil (aa 248-277, in *Y. enterocolitica* [54]); AD, amphiphatic domain (aa 278-292, in *Y. enterocolitica* [55]).

(g) YopD-ALFA associates with endogenous YopB. HeLa cells were pretreated with CNF-1 (condition WA-314 YopD-ALFA) or left untreated (WA-314) and infected and digitonin lysed. Cleared lysates were subjected to pulldown with NbALFA beads and lysates (L = lysate), supernatants (SN) and pull-down (PD) eluates were analyzed by Western blotting using anti-(α) YopD and anti-(α) YopB antibodies.

(h) STED microscopy confirms YopD-ALFA and YopB colocalization in infected HeLa cells. Hela cells were infected as in h (multiplicity of infection 10) and co-immunostained for YopD-ALFA and YopB. Scale bar: 1 µm.

(i) *Y. enterocolitica* strain expressing YopD-ALFA shows wild type effector translocation activity. HeLa cells were infected with *Y. enterocolitica* wild type strain WA-314 [24] and strain WA-314 YopD-ALFA in which endogenous YopD was substituted with ALFA-tagged YopD. After infection (multiplicity of infection 100) for 1 h, HeLa cells were lysed with digitonin and lysates were analyzed with Western blotting for translocated *Yersinia* effector YopH, ALFA-tag, pore forming *Yersinia* effector YopD and host cell protein calnexin as loading control.

Fig. 2 MINFLUX nanoscopy of *Y. enterocolitica* translocon protein YopD and sorting platform protein Halo-YscL.

(a) Comparison of STED-, STORM- and MINFLUX super-resolution microscopy of YopD-ALFA. Hela cells expressing Rac1Q61L were infected with WA-314 YopD-ALFA (multiplicity of infection 10) for 1 h and stained with NbALFA-Abberior STAR 635P or NbALFA-Alexa Fluor 647. **(i, iv, vii):** YopD-ALFA fluorescence signals co-recorded using STED-, STORM- or MINFLUX super-resolution microscopy with confocal or epifluorescence microscopy as indicated. Scale bar: 1 µm. **(ii, v, viii):** 10-fold magnifications of boxed areas in i,iv,vii. Scale bar: 100 nm. **(iii, vi, ix):** Intensity profiles for super-resolution nanoscopy (green lines) or confocal/epifluorescence microscopy (red lines) along dashed lines in ii, v and viii. Fluorescence intensity is displayed in arbitrary units and was normalized to the maximal intensity of each individual imaging method.

(b) MINFLUX nanoscopy of ALFA-tagged YopD at single molecule level.

(Top row) YopD-ALFA fluorescence signals in single pore complexes recorded with MINFLUX nanoscopy. Scale bar: 25 nm. **(Bottom row)** Interpretation of the respective YopD-ALFA localizations in the top row assuming incomplete labeling of YopD-ALFA proteins and considering potential spatial orientations of the pore complexes. Scale bar: 25 nm.

(c) STORM and MINFLUX nanoscopy of sorting platform protein Halo-YscL.

Y. enterocolitica bacteria expressing Halo-tagged YscL (Halo-YscL) were shifted to calcium-depleted medium at 37°C for 3 h to activate T3SS secretion and then stained with Alexa Fluor 647-labeled Halo substrate.

(Top row) Epifluorescence microscopy (i) and STORM (ii, iii) nanoscopy of Halo-YscL. Boxed area in (ii) (Scale bar: 200 nm) is magnified 10-fold in (iii) (Scale bar: 20 nm). (iv): Bottom view of schematic representation of the Halo-YscL complex in the sorting platform (scale bar: 4 nm), derived from [4].

(Bottom row) Confocal microscopy (v) and MINFLUX (vi, vii) nanoscopy of Halo-YscL. Boxed area in (vi) (Scale bar: 200 nm) is magnified 10-fold in (vii) (Scale bar: 20 nm). (viii): Interpretation of the YscL-Halo localizations considering the expected size of a YscL-Halo dodecamer depicted in (iv).

Fig. 1

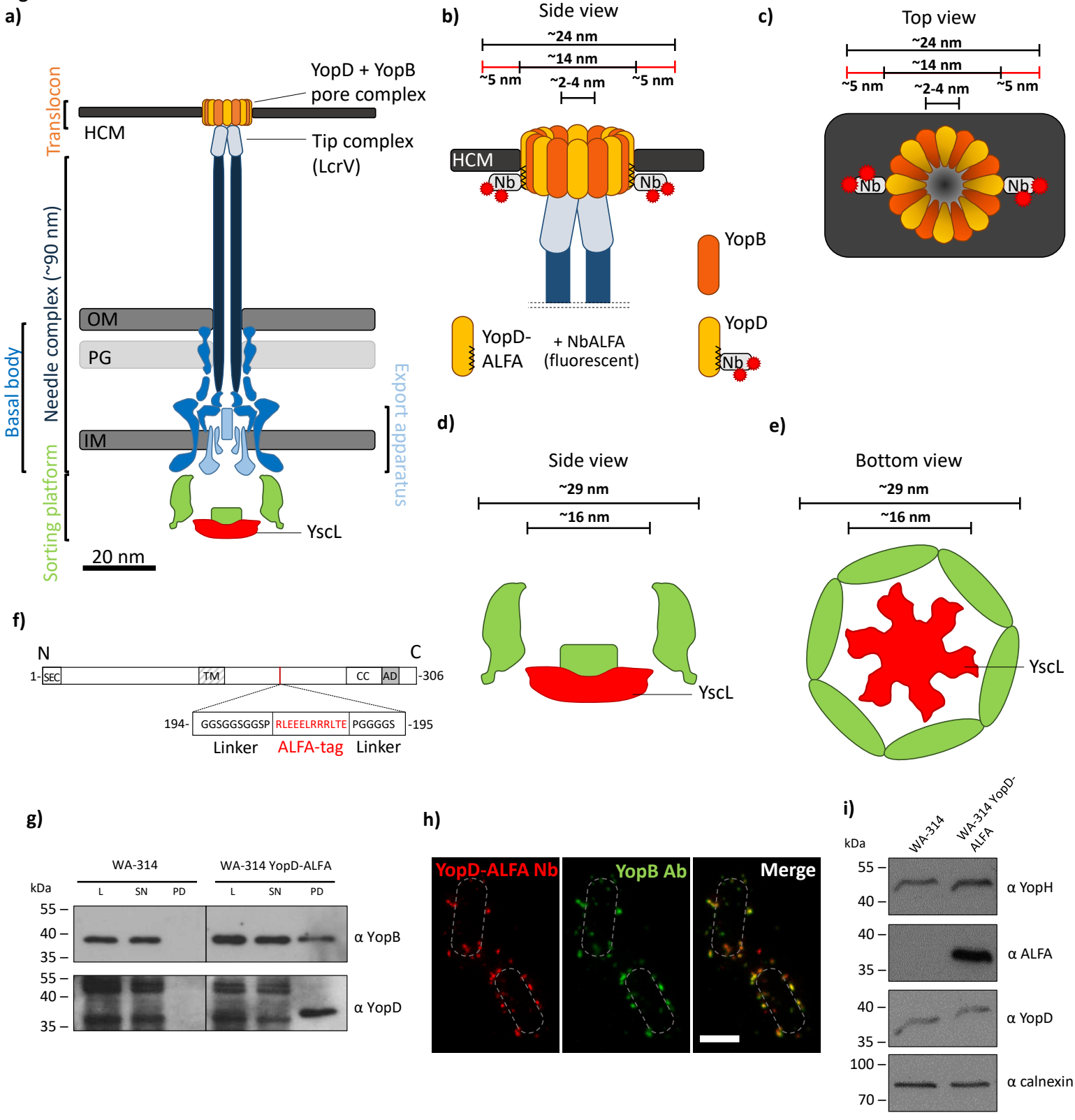

Fig. 2